Rheological properties of enzymatic milk gel: Effect of ion partitioning in casein micelles

Julien Bauland, Marie-Hélène Famelart, Marc Faiveley, Thomas Croguennec

Food Hydrocolloids 130 (2022) 107739

Contents lists available at ScienceDirect

Food Hydrocolloids

journal homepage: www.elsevier.com/locate/foodhyd

Rheological properties of enzymatic milk gel: Effect of ion partitioning in casein micelles

Julien Bauland [a,b], Marie-Hélène Famelart [a], Marc Faiveley [b], Thomas Croguennec [a,*]

[a] INRAE, Institut Agro, STLO, 35042, Rennes, France
[b] Chr. Hansen, 2970, Hoersholm, Denmark

ARTICLE INFO

Keywords:
Casein micelle
Minerals
Colloidal gel
Rheology
Milk gel
Structure

ABSTRACT

Casein micelles (CMs) are colloids of ~150 nm diameter formed by the association of milk proteins and minerals. Divalent milk cations, i.e. Ca^{2+} and Mg^{2+}, exist in two forms in CMs: either directly bound to casein residues (C-bound) without inorganic phosphate, or in a precipitated form called micellar calcium phosphate (MCP). The composition and properties of CMs vary with changes of the physicochemical conditions of milk; e.g. after the addition of salt or a change of pH. Moreover, the rheological properties of enzymatic milk gels are known to be strongly influenced by variations of mineral equilibria. We report in this study on the effect of cation partitioning in CMs on the rheology of enzymatic milk gel. Firstly, salts and acid ($CaCl_2$, $MgCl_2$, Na_2HPO_4, Na_3Cit and HCl) were added to produce a set of 19 milk samples containing different proportions of C-bound and MCP in order to identify correlations with rheological parameters (G′, G″, tanδ) of the resulting gels. Three milks were then selected according to the mineral content of CMs and the resulting gels were further characterized in order to propose mechanisms that might explain the dependence of gel macroscopic properties on those of CMs. We showed that the rheological properties of gel were well correlated with the two types of cations present in CMs: an increase in C-bound cations raised the values of G′ and G″ while an increase in the MCP content lowered the tanδ. To explain these inter-dependencies, CMs were viewed as soft colloids whose modulus could be tuned by their MCP content. Consequently, CMs with different mineral contents would have differing abilities to fuse after aggregation, which appeared to link the rheological and microscopic attributes of the gels in a consistent manner. These results will be useful to understand the complex variations in the rheological properties of milk gels produced in the dairy industry.

1. Introduction

Caseins are phosphorylated proteins characteristic of mammal milks (Holt, 2016). With milk minerals (mainly calcium and inorganic phosphate) they form spherical colloidal structures called casein micelles (CMs). CMs display a size distribution of around ~150 nm in bovine milk. Minerals account for 7% (w/w) of the dry mass of CMs under physiological conditions (Fox & Brodkorb, 2008; McMahon & Oommen, 2013). Divalent cations in CMs (mainly Ca^{2+} but also Mg^{2+}) are present in two forms. Most micellar calcium is associated with inorganic phosphate in tiny granules called "nanoclusters" (Holt, 1992), or micellar calcium phosphate (MCP). MCP nanoclusters are sequestered by multi-phosphorylated clusters on the primary structure of caseins which control the precipitation of calcium phosphate in milk. Each nanocluster is stabilized by the phosphoserine clusters of several caseins that also establish non-specific interactions between their hydrophobic regions. To simplify the ongoing debate on the internal structure of CMs (Holt, Carver, Ecroyd, & Thorn, 2013; D.S.; Horne, 2020), they can be seen as micro-gels containing thousands of casein monomers and ~200 nanoclusters (Holt & Carver, 2022). The equilibrium of MCP with soluble calcium phosphate in the aqueous phase depends on the saturation index of the latter. Some Ca^{2+} and Mg^{2+} are also directly associated with phosphoserine, glutamic and aspartic residues, without inorganic phosphate (Holt & Carver, 2022; Holt, Davies, & Law, 1986). The amount of these cations directly bound to caseins (C-bound) depends on the ionic activity of their free form in the soluble phase. C-bound caseins were found to be of particular importance in a recent model of CM (Holt & Carver, 2022) where a significant fraction of caseins is "free", i.e. not directly bound to nanoclusters. Consequently, C-bound would have cross-linking and charge neutralizing effects between caseins.

* Corresponding author.
E-mail address: thomas.croguennec@agrocampus-ouest.fr (T. Croguennec).

https://doi.org/10.1016/j.foodhyd.2022.107739
Received 17 January 2022; Received in revised form 1 April 2022; Accepted 13 April 2022
Available online 16 April 2022

Mineral equilibria are of considerable importance when dealing with CMs, as a minor modification of mineral distribution can markedly modify the properties and stability of the colloids (Bauland et al., 2020; Philippe, Le Graët, & Gaucheron, 2005). It is worth noting that little is known about newly formed MCP after the addition of $CaCl_2$ or Na_2HPO_4, regarding either its composition or its interactions with caseins (Gaucheron, 2004). It was recently suggested that the nanoclusters may grow in size to accommodate precipitating MCP (Wang, Holt, Nylander, & Ma, 2020).

The colloidal stability of CMs arises from κ-casein, which is located at the surface of the colloid. Its highly hydrophilic C-term part protrudes into the medium and supplies steric and electrostatic repulsions (De Kruif, 1999). Altering the state of the κ-casein layer destabilizes CMs and can lead to the formation of a colloidal gel. This process has been used empirically for centuries in the manufacture of yogurt and cheese. During the latter, a proteolytic enzyme is added to the milk; it specifically hydrolyzes κ-casein and produces the complementary part called para-CMs (Horne & Lucey, 2017). After substantial hydrolysis, para-CMs start to aggregate and gelation occurs through a diffusion-controlled process, limited by intermediate range repulsive interactions (Horne & Lucey, 2014; Mellema, Van Opheusden, & Van Vliet, 1999). The resulting colloidal gel belongs to the category of weak physical gels, formed by non-covalent interactions. Interactions between para-CMs are likely to be of the same nature as those involved in the internal structure of CMs (Horne, 1998). A particular feature of enzymatic milk gel is its transient character and its ability to display micro- and macro-syneresis (Mellema, Walstra, van Opheusden, & van Vliet, 2002; van Vliet, van Dijk, Zoon, & Walstra, 1991; Walstra, van Dijk, & Geurts, 1985). Indeed, para-CMs are supposed to be reactive throughout their surface and this process can range from touching at the onset of gelation to fusion during aging (van Vliet et al., 1991). The increasing number of bonds between colloids, at the origin of endogenous stress within the casein network, is responsible for a state of non-equilibrium and for rearrangement of the gel structure over time. This rearrangement can occur at different stages, from particle fusion to strand breaking, and is responsible for an increase in the shear modulus of the gel (Mellema, Walstra, et al., 2002).

The rheological properties of enzymatic milk gel have been studied extensively (Mishra, Govindasamy-Lucey, & Lucey, 2005; Vilet, Roefs, Zoon, & Walstra, 1989; Zoon, 1988). Particular attention has been given to the content and distribution of minerals in milk insofar as they affect enzymatic coagulation and gel properties. Under most conditions, increasing the level of micellar calcium increases the shear moduli of the gel at a given frequency (Cooke & McSweeney, 2014; Udabage, McKinnon, & Augustin, 2001; Zoon, 1988), while decreasing it has the opposite effect (Choi, Horne, & Lucey, 2007). However, this observation is not always true. For example, a small reduction in the milk pH reduces the amount of micellar calcium but also increases the shear moduli of the enzymatic gel (Choi et al., 2007). Udabage et al. (2001) added various salts to milk and measured the G′ value 3 h after addition of the coagulant. They highlighted the significance of Ca^{2+} activity, the MCP content and the proportion of caseins in CMs but without attributing a distinctive role to each. Zoon, van Vliet, and Walstra (1988) investigated the respective relevance of MCP and bound-Ca under various dialysis conditions and in artificial micelle preparations to obtain different proportions of the two calcium forms in CMs. They concluded that tanδ was negatively correlated to the MCP content and that G′ and G″ increased in line with Ca^{2+} activity from a minimal MCP content. Other authors also reported on tanδ being negatively correlated to the MCP content, particularly at a low frequency (Choi et al., 2007; Cooke & McSweeney, 2014) without giving any explanations for this dependency. Zoon et al. (1988) suggested that the MCP content might be directly linked to the viscoelastic properties of the gel by affecting the number of bonds with a long relaxation time. They also suggested that this effect could be indirect if the MCP content changed the CM sub-structure and other types of interactions. Choi et al. (2007) assumed that a reduction in micellar calcium levels would loosen the CM structure and lead directly to a weaker and more flexible network. High (or low) tanδ values would reflect more (or less) fluid-like properties for the CMs and a higher (or lower) propensity of para-CMs to fuse and subsequent rearrangement of the network, as suggested by Mellema, Walstra, van Opheusden, and van Vliet (2002) and supported by Cooke and McSweeney (2014). However, this does not explain why the dynamic properties of the enzymatic gel at a given time would depend on the MCP content in CMs and which levels of the gel structure need to be considered to explain differences in its rheological properties following changes of mineral equilibria. As pointed out by Mellema, Walstra, et al. (2002), there is a lack of information on how the properties of CMs affect the macroscopic properties of the gel.

In this paper, the mineral content of CMs was modified by adding various concentrations of salts and acid ($CaCl_2$, $MgCl_2$, Na_2HPO_4, Na_3Cit and HCl) to milk in order to establish a general link between partitioning of the two forms of cations in CMs (C-bound and MCP) and the rheological properties of the enzymatic gel (part 3.1). Three samples were then selected regarding ion partitioning in CMs and analyzed at different spatial and time scales in order to reveal mechanisms which might explain the dependency of gel macroscopic properties on the properties of CMs (part 3.2).

2. Materials and methods

2.1. Materials

Low-heat skimmed milk powder, to use as a model milk system, was prepared in-house. More information on production of this powder can be found elsewhere (Bauland et al., 2020). $CaCl_2.2H_2O$, Na_2HPO_4, NaN_3, Fast Green FCF, glutaraldehyde solution (25%) and sodium cacodylate trihydrate were purchased from Sigma-Aldrich (St. Louis, MO). $MgCl_2.6H_2O$ came from Merck (Darmstadt, Germany) and KCl was purchased from PanReac (Lyon, France). $Na_3Cit.2H_2O$ was obtained from Carlo Erba (Val-de-Reuil, France), while NaOH and HCl were purchased from VWR International (Fontenay-sous-Bois, France). The coagulant was a fermentation-produced camel chymosin (CHY-MAX® SUPREME 1000 international milk clotting units (imcu).mL^{-1}, Chr. Hansen, Horsholm, Denmark).

2.2. Milk sample preparation

Skimmed milk was prepared by rehydrating the low-heat skimmed milk powder at 110 g.L^{-1} in ultrapure water with the addition of 0.2 g.L^{-1} NaN_3 as bio-preservative. The reconstituted skimmed milk was stirred for 2.5 h at room temperature and salts were added from 1 M stock solutions (except for Na_2HPO_4 added from a 0.5 M stock solution). If required by the experimental design (see Table 1), the pH was adjusted to pH 6.65 using 1 M NaOH or HCl solutions and the milk samples were left overnight at room temperature to achieve equilibration. The pH was then adjusted again if necessary and the samples were diluted to 100 g.L^{-1} (29 g.L^{-1} caseins) by adding the appropriate amount of ultra-pure water. The samples were finally left to equilibrate at 30 °C for 30 min before analysis.

2.3. Mineral equilibria

Contents in micellar calcium phosphate (MCP), divalent cations (Ca^{2+} and Mg^{2+}) bound to caseins (C-bound) and free divalent cations (C-free) in the milk samples were calculated using MILK SALT GLM software (Mekmene, Le Graët, & Gaucheron, 2009) which models mineral equilibria in milk at 20 °C using the total ion concentrations and casein content determined experimentally, together with the milk pH. This approach has been validated (Mekmene et al., 2009), notably for this particular milk system (Bauland et al., 2020). The ion activity coefficients are calculated from the ionic strength value and the distribution of ions in and between the soluble and micellar phases of milk, using

Table 1
Variations of pH, free cations (C-free) and the two forms of micellar cations (C-bound and MCP) in milk samples and associated rheological properties of the gels.[a].

Additions	pH	C-free (mM)	C-bound (mM)	MCP (mM)	$tan\delta_{0.9Hz}$	$tan\delta_{0.03Hz}$	G' (Pa)	G'' (Pa)
Standard	6.65	2.4	5.0	21.6	0.251	0.469	67	20
2.5 mM $CaCl_2$	6.60	2.8	5.3	23.3	0.248	0.447	91	26
5 mM $CaCl_2$	6.50	3.4	5.6	24.6	0.248	0.424	77	22
10 mM $CaCl_2$	6.30	5.4	6.2	26.5	0.243	0.407	93	26
2.5 mM $CaCl_2$[b]	6.65	2.7	5.3	23.5	0.247	0.446	91	27
5 mM $CaCl_2$[b]	6.65	3.0	5.5	25.3	0.244	0.425	93	26
10 mM $CaCl_2$[b]	6.65	4.0	6.0	28.5	0.239	0.390	97	27
HCl_6.6	6.60	2.5	5.1	21.4	0.250	0.469	82	24
HCl_6.5	6.50	2.7	5.2	21.0	0.255	0.463	90	27
HCl_6.3	6.30	3.4	5.4	19.9	0.255	0.461	90	26
HCl_6.0	6.00	5.0	5.7	17.5	0.270	0.498	92	28
2.5 mM Na_2HPO_4[b]	6.65	2.0	4.6	22.5	0.251	0.477	67	20
5 mM Na_2HPO_4[b]	6.65	1.8	4.3	23.2	0.251	0.479	70	21
10 mM Na_2HPO_4[b]	6.65	1.5	3.7	24.4	0.250	0.495	66	20
2.5 mM $MgCl_2$	6.60	3.2	5.6	22.3	0.250	0.449	93	27
5 mM $MgCl_2$	6.50	4.4	6.1	22.5	0.248	0.448	106	31
10 mM $MgCl_2$	6.40	7.2	6.9	22.7	0.247	0.447	110	31
10 mM $MgCl_2$[b]	6.65	6.2	6.8	24.0	0.245	0.433	114	33
2.5 mM Na_3Cit[b]	6.65	2.0	4.8	20.2	0.256	0.490	61	19

[a] Mean value of duplicate.
[b] Indicates that the pH was corrected to 6.65 ± 0.03. C-free and C-bound mean the sum of Ca^{2+} and Mg^{2+} in the aqueous phase or directly bound to phosphoserine residues of caseins, respectively. MCP is micellar calcium phosphate. G′ and G″ are the values of the elastic and viscous moduli, respectively, taken at $t = 4 \times t_{gel}$. $tan\delta_{0.9Hz}$ and $tan\delta_{0.03Hz}$ are the values of the loss tangent at 0.9 and 0.03 Hz determined at 120 min after addition of the coagulant.

their respective affinity constants. The algorithm works by successive iterations until the ionic strength is constant and the concentration of soluble $CaHPO_4$ is 0.6 mM, as set by Mekmene et al. (2009).

2.4. Rheological measurements

Rheological measurements were performed using a stress-controlled rheometer (MCR 301, Anton Paar) equipped with either CC39 (cup diameter = 42.02 mm, bob diameter = 39.00 mm) or CC17 (cup diameter = 18.08 mm, bob diameter = 16.66 mm) coaxial cylinders, used for parts 3.1 and 3.2, respectively.

Milk samples were stored at 30 °C during the 30 min prior to analysis and the measurements were carried out at this temperature.

For part 3.1, the coagulant was added to the milk at a final concentration of 0.05 imcu.mL^{-1} and a volume of 40 mL of milk + coagulant was loaded into the geometry and covered with paraffin oil. Gel formation was monitored over 5 h (frequency $f = 0.1$ Hz, shear strain $\gamma = 0.01$) before initiating a frequency sweep from 1.6×10^0 to 1.6×10^{-3} Hz (4 points/decade, $\gamma = 0.01$). The gelation time (t_{gel}) was determined arbitrarily when $G' = 1$ Pa.

For part 3.2., the coagulant concentration was reduced and adjusted to produce a similar t_{gel} for the three selected milk samples. Thus, 0.020, 0.010 and 0.014 imcu.mL^{-1} of coagulant were added to the samples at pH 6.6, at pH 6.0 and supplemented with 10 mM $CaCl_2$ (referred to as control, acidified and calcium-fortified) respectively, and a volume of 4.5 mL milk + coagulant was loaded into the geometry and covered with paraffin oil. Gel formation was monitored for up to 40 h ($f = 0.1$ Hz, $\gamma = 0.01$). A frequency sweep (3×10^0–1.6×10^{-3} Hz, $\gamma = 0.01$) was initiated at either a fixed time of 5 h (1.8×10^4 s) after coagulant addition or when G′ reached its maximum value G'_{max}. A creep test (stress $\sigma = 0.5$ Pa, $t = 1.08 \times 10^4$ s) was also initiated when $G' = G'_{max}$. These procedures ensured that G′ and G″ would vary by no more than 1 Pa throughout the duration of the creep and frequency sweep tests. A stress sweep (0.1–10^3 Pa, $f = 1$ Hz) performed at 5 h after coagulant addition (data not shown) revealed that the strain was proportional to the strain up to $\gamma = 0.02$–0.03 and $\sigma = 4$–5 Pa.

Creep data were fitted using a fractional Maxwell model consisting of a spring and a spring-pot in series (Aime, Cipelletti, & Ramos, 2018):

$$J(t) = \frac{1}{G_0}\left[1 + \frac{1}{\Gamma(\alpha+1)}\left(\frac{t}{\tau}\right)^{\alpha}\right] \quad (1)$$

with J(t) the creep compliance (Pa^{-1}), t the time (s), G_0 the elastic instantaneous modulus (Pa) and τ a characteristic time (s). The power exponent α ranged from 0 to 1 and reflected the viscoelastic character of the spring-pot, the two limiting cases being $\alpha = 0$ for a pure elastic spring and $\alpha = 1$ for a pure viscous dashpot.

Creep data were fitted using the Matlab curve fitting toolbox (version 9.10.0.1602886 R2021a).

2.5. Confocal laser scanning microscopy and image analysis

Confocal laser scanning microcopy (CLSM) images were acquired on an inverted Zeiss LSM 880 microscope (Carl Zeiss SAS, Marly Le Roi, France). Proteins were labeled 2 min before addition of the coagulant by adding Fast green FCF (10 g.L^{-1} stock solution in water) to the milk to obtain a final concentration of 0.012 g.L^{-1} (Ong, Dagastine, Kentish, & Gras, 2010). After coagulant addition, 400 μL milk were loaded into the well of a chamber slide (uncoated μ-Slide 8 well, Ibidi) and covered with 200 μL paraffin oil. The slide was immediately placed on a × 63 oil-immersion objective (NA = 1.4) in the thermo-regulated chamber of the microscope set at 30 °C. A He/Ne laser with a wavelength of 633 nm was used and image acquisition was achieved using the Airyscan detector in super resolution mode with the zoom set at 1.8. Laser power (10% of the maximum), gain (820) and pixel dwell time (6.18 μs) were kept constant for all images. Images were acquired at 20 μm from the slide. Four images of 1336 × 1336 $pixel^2$ (73.5 × 73.5 μm^2) were acquired automatically on four different areas every 10 min over 120 min. Beyond 120 min, the gels tended to exhibit some macro-syneresis, detected easily on the images from a shift of the structure in the XY plan from one image to another. Macro-syneresis, which does not occur in a rheometer, was observed using either glass or uncoated plastic slides. To ensure the lack of any macro-syneresis during the observation period, the latter was thus limited to 120 min. Zen Black 2.1 software (version 13.0.0.0) was used to process the images using the default settings of the Airyscan processing function. The software processed the 32 Airy detector channels to supply images with an enhanced signal to noise ratio.

The characteristic size of the gel pores was calculated from the CLSM images using grey level granulometry with Matlab and the plugin granulomorphogui.m available for downloading at https://www.pfl-cepia.inra.fr/index.php?page=granulomorphogui_en. The methodology for calculation can be found in the article by Legland, Devaux,

Bouchet, Guillon, and Lahaye (2012). Briefly, the plugin enables the operation of mathematical transformations such as morphological closings or openings using a mask called a "structuring element". During a closing operation, dark objects (i.e. with low grey level intensities such as the pores of the gel) that are smaller than the structuring element disappear. By performing *i* successive closing operations while increasing the size of the structuring element with a step ε, it is possible to calculate the sum of grey level intensities V(i) at each closing step. A granulometric curve g(i), similar to a distribution, is obtained by plotting the change in grey level intensity at each closing step, i.e. V(i) - V(i + ε), normalized by the initial and final sum of grey levels V_0 and V_f:

$$g(i) = \frac{V(i) - V(i+\varepsilon)}{V_0 - V_f} \quad (2)$$

For each curve, the geometric mean m was calculated as the following weighted sum:

$$m = \exp\left(\sum_i \frac{g(i) \times \log(\xi)}{100}\right) \quad (3)$$

where ξ was the size of the structuring element in μm.

The geometric mean usually corresponds to the distribution mode, and was taken as the characteristic size of the gel pores. A square structuring element ranging from 1 to 100 pixels with a step of 1 was used to perform closing operations. Based on the distribution of grey level intensities, this image analysis methodology did not require image thresholding prior to calculation.

The evolution of gel pore sizes over time was fitted with an empirical growth model ($R^2 > 0.983$) to guide the eye:

$$f(t) = a \times \left(1 - \exp\left(\frac{b}{t}\right)\right) + c \quad (4)$$

with f(t) the size of gel pores (μm), t the time (s) and a, b and c some adjustment constants.

2.6. Scanning electron microscopy

The coagulant was added to 100 ml milk at 30 °C as described in 2.4 and small cylindrical plastic tubes (diameter~2 mm, height~1 cm, obtained by cutting sections of plastic pipettes) were immediately placed in the milk and remained there during coagulation. 120 min after coagulant addition (i.e. no macro-syneresis), the tubes filled with gel were gently harvested. They were immersed immediately in the fixation solution for 24 h at 20 °C and the gel was then gently pushed out of the tubes. This procedure limited gel handling before fixation. The fixation solution consisted of 2.5% (v/v) glutaraldehyde in 0.1 M sodium cacodylate buffer equilibrated at pH 7.2 (Famelart, Tomazewski, Piot, & Pezennec, 2004). The samples were then rinsed thoroughly with ultrapure water and dehydrated in successive graded ethanol baths (20, 40, 60, 80, 96, 100%) for periods of 30 min at each concentration. They were then dried at the CO_2 critical point using a Leica EM CPD300 (Leica Microsystems, Vienna, Austria), fractured and then gold sputter-coated using a Leica EM ACE200. Scanning electron microscopy (SEM) observations were performed with a JEOL-JSM-7100F (JEOL USA Inc., Peabody, USA). The overall sample preparation and observation procedures were repeated twice, and representative images are presented herewith.

2.7. Statistics

All statistical analyses were performed using RStudio Team 2018 (RStudio: Integrated Development for R. RStudio, Inc., Boston, http://www.rstudio.com). Multiple mean comparisons were made using one-factor analysis of variance (risk $\alpha = 0.05$) followed by a Tukey test. If the homogeneity of variance was rejected, a Kruskal-Wallis test and then a Dunn test were performed. Principal component analysis (PCA) was performed using the FactoMineR and Factoshiny packages (Lê, Josse, & Husson, 2008).

3. Results and discussion

3.1. Direct link between the dynamic rheological properties of enzymatic milk gels and the partitioning of cations in casein micelles

In this first part of the study, a set of milk samples with CMs containing different proportions of MCP and C-bound was obtained by selective additions to a standard milk of salts and/or changes of pH (Table 1). The MCP and C-bound contents were calculated from the total ion concentrations using MILK SALT GLM (see part 2.3). The dataset was described using PCA (Fig. 1) in order to identify any correlations between the rheological properties of gels and the MCP and C-bound contents in CMs, independently of other variables such as pH, soluble casein concentrations or the hydration degree of CMs. Among the variables displayed, the G′ and G″ values determined at $t = 4 \times t_{gel}$ correlated positively to the C-bound content whereas tanδ, at either 0.3 or 0.9 Hz, was negatively correlated to both the MCP and total content of divalent cations in CMs. For example, the addition of $CaCl_2$ to milk increased levels of both MCP and C-bound, and the resulting gels displayed higher G′ and G″ values at $4 \times t_{gel}$ and a lower tanδ compared to the standard (Table 1). Adding $MgCl_2$ also increased the MCP and C-bound contents, but the increase in MCP was smaller compared to the same addition of $CaCl_2$. Consequently, the gels formed with $MgCl_2$ showed increases in G′ and G″ and a decrease in tanδ versus the standard, but the decrease of tanδ was smaller when compared to the same addition of $CaCl_2$. On the other hand, adding Na_3Cit decreased both types of micellar cations, resulting in decreases in G′ and G″ and an increase in tanδ. The first and second principal components explained ~92% of dataset variability, indicating that under the given set of conditions, the rheological properties of the gels correlated well to the partitioning of cations in CMs.

The maximum G′ and G″ values obtained by fitting the 120 min time

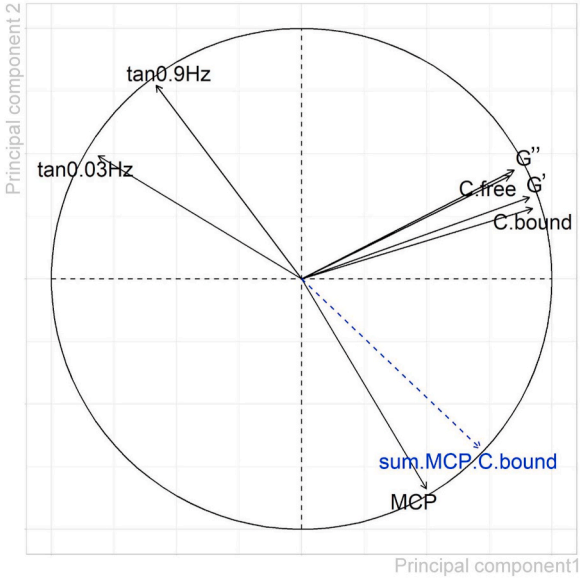

Fig. 1. Principal component analysis (PCA) of cation partitioning in casein micelles (CMs) and the dynamic rheological properties of enzymatic milk gels (data set of Table 1). C-free and C-bound mean the sum of Ca^{2+} and Mg^{2+} in the aqueous phase or directly bound to phosphoserine residues of caseins, respectively. MCP is the micellar calcium phosphate. G′ and G″ are the value of the elastic and viscous moduli of the gel taken at $t = 4 \times t_{gel}$. $tan\delta_{0.9Hz}$ and $tan\delta_{0.03Hz}$ are the values of the loss tangent of the gel at 0.9 and 0.03 Hz determined at 2 h (7.2×10^3 s) after coagulant addition.

sweep with the empirical growth model developed by Scott Blair & Burnett (see Supplementary Information), was also positively correlated with the C-bound content in CMs. This suggests that the positive correlation between the C-bound content and G′ and G″ values was valid within a broad range of the gel firming kinetics. The absolute values of G′ and G″ are reliant on the total number of bonds between para-CMs (Horne & Lucey, 2017). Therefore, the positive correlation between G′ and G″ and the C-bound content probably resulted from shielding of the CM negative charges following the association of divalent cations with free phosphoserine residues and carboxylate groups on the primary structure of caseins. Ca^{2+} and Mg^{2+} are counter-ions with a high affinity for these residues within the pH range covered during this study. Changes of the colloid charge might favor or hinder bond setting when para-CMs start to aggregate and also after t_{gel}, affecting the viscoelastic moduli of the enzymatic gel. This hypothesis agrees with that advanced by Zoon (1988) who reported that the G′ and G″ values depend on the Ca^{2+} activity for a minimal MCP content.

The tanδ value was negatively correlated to the MCP content and to the total concentration of cations in CMs, MCP being the most abundant form. This means that the enzymatic gel has a more viscous contribution and a more elastic contribution to the strain response at low and high MCP contents in CMs, respectively. This link had previously been observed, either when decreasing (Choi et al., 2007) or increasing (Cooke & McSweeney, 2014) the MCP content, and was confirmed here with various types of cation partitioning in CMs, suggesting a general trend. Explaining this link between gel rheology and intra-micellar interactions is not straightforward. As pointed out by Zoon (1988), colloid rigidity may directly contribute to gel rheology and a higher degree of crosslinks in the internal structure of CMs as the result of a higher MCP content increasing the number of bonds with a high relaxation time. However, enzymatic milk gel has been shown to be formed through cluster-cluster aggregation and different levels of the structure, such as strands and clusters, have been described as contributing to gel rheology (Mellema, van Opheusden, & van Vliet, 2002). By comparing enzymatic milk gels made at pH 6.6 and pH 5.3, Mellema, Walstra, et al. (2002) explained that a high tanδ value is indicative of a more fluid-like behavior of para-CMs after MCP removal. This would favor fusion between particles and enhance gel rearrangements, as suggested by the rapid loss of fractal organization at pH 5.3. Following the same idea, Cooke and McSweeney (2014) explained that a higher number of nanoclusters in CMs following the addition of $CaCl_2$ might limit particle fusion. However, the degree of particle fusion has not been assessed under the conditions described above and the link between the viscoelastic character of the gel and the MCP content in CMs remains unclear.

It should be noted that the addition of Na_2HPO_4 did not fully comply with the relationship described above. It reduced C-bound but G′ and G″ values remained somewhat constant at $4 \times t_{gel}$. Tanδ values rose slightly after the addition of 2.5 mM and remained constant at 5 and 10 mM, while the MCP content continued to increase. A similar evolution of the gel tanδ following an increase in the concentration of the added Na_2HPO_4 was reported by Udabage et al. (2001). This highlights the fact that we know little about newly formed MCP and how it interacts with caseins. Unlike the current study, Udabage et al. (2001) observed an increase in G′ and G″ values after the addition of Na_2HPO_4.

In the following section, our aim was to investigate the relevance of the MCP-dependent fusion of para-CMs in order to explain the different rheological properties and structures of enzymatic milk gels during aging. To achieve this, a set of three samples with different MCP contents, namely: i) "control" corresponding to HCl_6.6 in Table 1: milk without any added salt and adjusted to pH 6.6; ii) "acidified" corresponding to HCl_6.0 in Table 1: milk without any added salt and adjusted to pH 6.0; iii) "calcium-fortified" corresponding to 10 mM $CaCl_2$ in Table 1: milk with 10 mM $CaCl_2$ added and without pH correction (pH 6.3), were further characterized for their rheological properties in the linear domain and using CLSM and SEM. The control sample was chosen as a reference regarding its MCP and C-bound contents. The calcium-fortified and acidified samples both had CMs that displayed an increase in their C-bound content but an increase of 24% and a decrease of 18% in their MCP content, respectively (Table 1).

3.2. *Effect of the calcium phosphate content in casein micelles on the aging kinetics and the rheological properties of enzymatic milk gels (control, acidified and calcium-fortified samples)*

3.2.1. *Dynamic and transient rheological properties*

The gelation kinetics of control, acidified and calcium-fortified samples, recorded over 40 h (1.44×10^5 s) after addition of the coagulant, are shown in Fig. 2A. After passing through a maximum, G′ and G″ decrease, as previously reported (Choi et al., 2007). The inset in Fig. 2A reveals that tanδ was not constant after gel setting, contrary to what has been reported for enzymatic milk gel (Horne & Lucey, 2017). The value reached a minimum under all conditions, corresponding to a time when the moduli attained 40–60% of their maximum values, and then slowly declined, indicating a transition of the gel towards more viscous-like behavior. The minimum tanδ value rose in line with the decrease in the MCP content in CMs, which was consistent with the results described in section 3.1 and the tanδ value measured during frequency sweeps (Table 1).

To better compare the aging kinetics between samples, G′ was normalized by its maximum value G'_{max} and plotted as a function of time normalized by the t_{gel} (Fig. 2B). The aging kinetics of the acidified sample was more rapid, while they were identical for the control and calcium-fortified samples up to ~5 times the t_{gel}, at which point the kinetics of the calcium-fortified sample slowed down. The decline of G′ after reaching its maximum value occurred sooner for the acidified

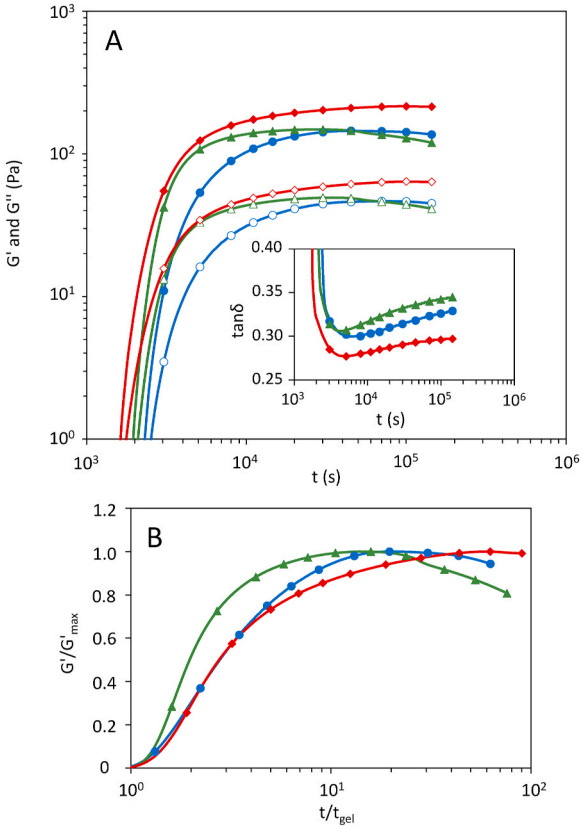

Fig. 2. (A) G' (close symbols) and G'' (open symbols) as a function of time after coagulant addition to milk (T = 30 °C, γ = 0.01, f = 0.1 Hz) for control (circles), acidified (triangles) and calcium-fortified (diamonds) gels. Inset displays tanδ on the same time interval. (B) Evolution of G′ normalized by its maximum value G'_{max} as function of time normalized by the gelation time t_{gel}.

sample and was delayed for the calcium-fortified sample, when compared to the control.

Fig. 3A shows the G′ and G″ values of the three samples (control, acidified and calcium-fortified) as a function of frequency, obtained 5 h (1.8×10^4 s) after addition of the coagulant. In all samples, G′ almost displayed a power law dependency with frequency: $G'(f) = G_0 \times f^{\alpha}$ with $\alpha \sim 0.2$. This means that under stress, the gel displayed a continuous range of relaxation times. Fig. 3B shows the tanδ(*f*) values of the same samples at 5 h and when $G' = G'_{max}$. The time corresponding to $G' = G'_{max}$ is shown in Table 2 for each sample. As expected, tanδ increased when *f* decreases, i.e. when the time scale of the test increased. Unlike the acid milk gel, the enzymatic milk gel did not fully behave as a power law material, as tanδ would be frequency independent (Bonfanti, Kaplan, Charras, & Kabla, 2020; van Vliet et al., 1991). The inset in Fig. 3B shows tanδ(*f*) normalized by the tanδ(*f*) obtained with the control sample at 5 h. This highlights how the tanδ(*f*) of the other samples deviated from the reference condition. It can thus be seen that the differences in tanδ values between samples were greater at lower frequencies. Consistent with the increase in tanδ over time (inset in Fig. 2A), the frequency sweep shifted towards higher values during aging (i.e. between 5 h and the time when G'_{max} was reached).

To characterize gel rheology over longer time scales, creep compliance tests were initiated when $G' = G'_{max}$ (Fig. 4). Overall, the calcium-fortified sample displayed less compliance than the two other samples (inset on Fig. 4), in accordance with the higher G′ value measured in oscillation before initiation of the creep test (Fig. 2A). For all samples,

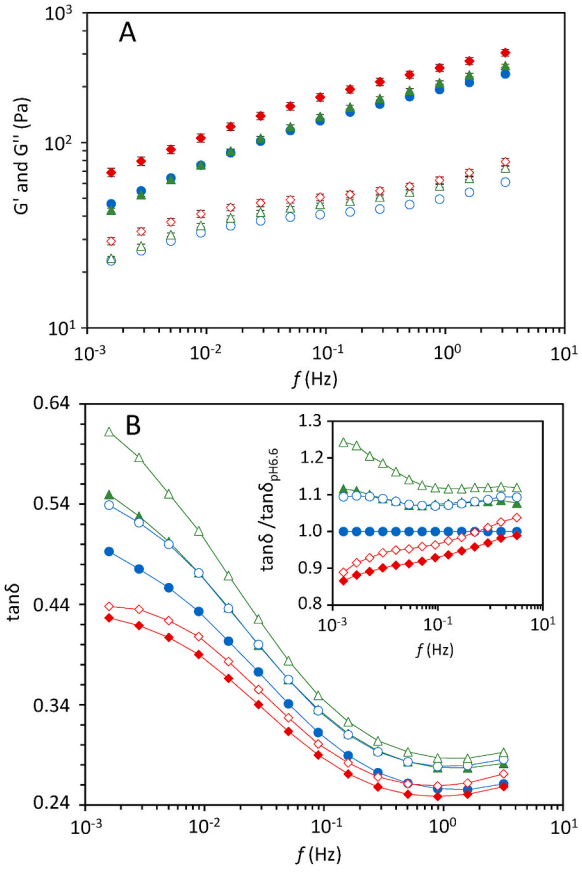

Fig. 3. (A) G' (close symbols) and G'' (open symbols) as a function of frequency (T = 30 °C, ɣ = 0.01) measured 5 h (1.8×10^4 s) after coagulant addition to milk for control (circles), acidified (triangles) and calcium-fortified (diamonds) gels. Means of triplicate ± standard deviation. (B) tanδ as a function of frequency measured 5 h (1.8×10^4 s) after coagulant addition to milk (open symbols) or when G′ reached its maximum value G'_{max} (close symbols). Inset displays tanδ divided by the tanδ of control gel at 5 h.

Table 2
Creep parameters of the fractional Maxwell model (equation (1) in part 2.4, $R^2 > 0.997$)[a].

Sample	Creep start time (s)[b]	α	G_0 (Pa)	τ (s)
control	36,000	0.37 ± 0.00	349 ± 4	1.0 ± 0.0
acidified	23,400	0.39 ± 0.01	380 ± 75	1.2 ± 0.4
calcium-fortified	79,200	0.26 ± 0.03	680 ± 400	0.3 ± 0.1

[a] Mean value of duplicate ± standard deviation.
[b] Time corresponding to $G' = G'_{max}$.

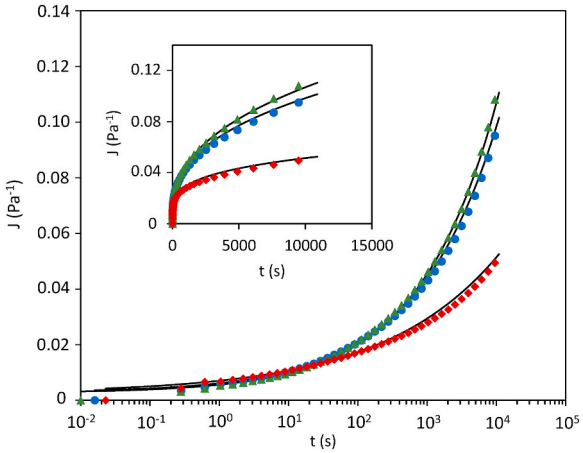

Fig. 4. Creep compliance curves (σ = 0.5 Pa) fitted with a fractional Maxwell model (continuous lines, $R^2 > 0.98$, see equation (1) in part 2.4) for control (circles), acidified (triangles) and calcium-fortified (diamonds) gels. The inset corresponds to the same graph with linear scales. Creep was initiated when G′ reached its maximum value G'_{max} and the strain was monitored during 3 h (1.08×10^4 s). For each sample, the time at which $G' = G'_{max}$ is displayed on Table 2.

the creep profile was well captured using a fractional Maxwell model (Fig. 4 and Table 2). This indicates that after instantaneous compliance, J evolved as a power law of time. Thus, at longer time scales, the gels did not completely flow but nor did they reach an equilibrium state. This confirms that the enzymatic gel contained no permanent network (Zoon, Roefs, de Cindio, & van Vliet, 1990). The lower α value found with the calcium-fortified sample indicates a stronger elastic behavior with a shorter characteristic time, whereas the control and acidified samples were more viscous. This was consistent with the frequency sweep results (Fig. 3B).

At 5 h following coagulant addition, the rheological properties of the gel obeyed the relationship proposed in part 3.1., and its viscoelastic behavior was negatively correlated to the MCP content in CMs. However, after a long aging time, dynamic and transient experiments showed that the calcium-fortified sample displayed a distinct elastic behavior, while during aging the control and acidified samples evolved toward a more viscous behavior. Because the interactions between para-CMs are supposed to continue to display the same nature during gel firming, these different rheological properties and aging pathways likely result from different kinetics of structure rearrangement.

3.2.2. *Gel microstructure assessed by CLSM and SEM*

The mesoscopic structure of the gels was observed using CLSM during 2 h (7.2×10^3 s) after addition of the coagulant (Fig. 5A–C). This period corresponded to ~4 times the t_{gel}, depending on the sample. The characteristic size of the pores was calculated from the micrographs using grayscale granulometry (Fig. 6). Interestingly, the evolution of pore size was similar in the control and calcium-fortified gels, while that of the acidified gel increases more rapidly and to a greater extent

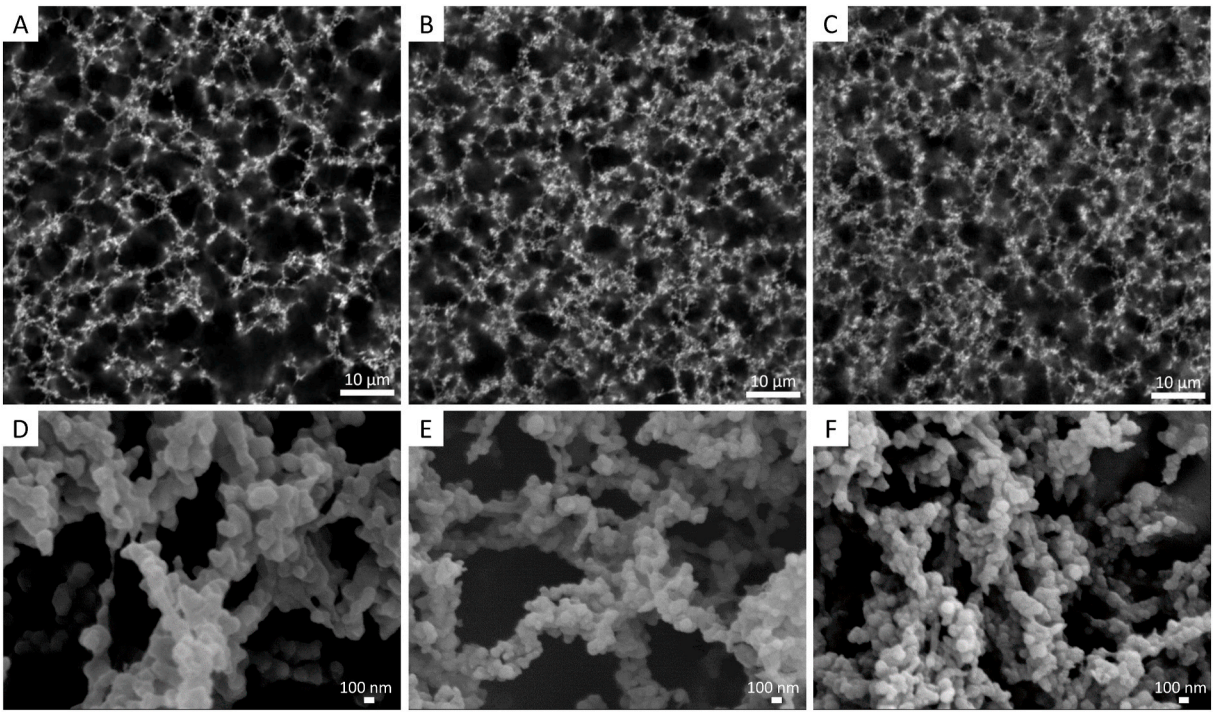

Fig. 5. Confocal (A–C) and scanning electron microscopy images (D–F) of acidified (A,D), control (B,E) and calcium-fortified (C,F) gels. Representative images, obtained 120 min (7.2×10^3 s) after coagulant addition to milk, are displayed.

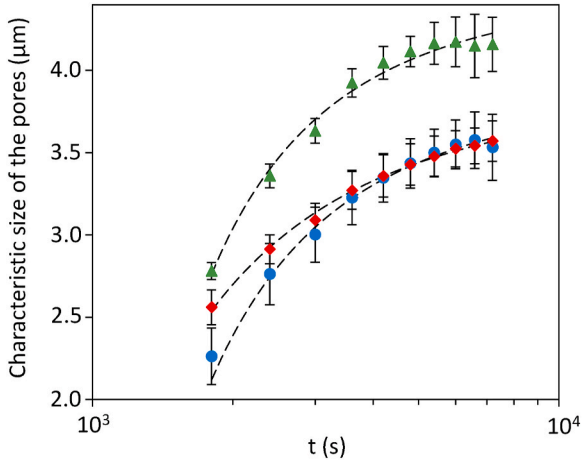

Fig. 6. Characteristic size of pores as a function of the time after coagulant addition to milk of control (circles), acidified (triangles) and calcium-fortified (diamonds) gels, determined from confocal images by grey level granulometry. Each time corresponds to 16 images from 4 different milk preparations. Means ± standard deviation are displayed. Kinetics are fitted with an empirical growth model (see equation (4) in part 2.5) to guide the eyes (dotted lines).

(Fig. 6). Two hours after coagulant addition, the acidified gel was indeed visually coarser than the other two (Fig. 5A–C). The aging kinetics of the three samples, assessed by both rheology (Fig. 3B) and CLSM (Fig. 6) were consistent between the two methods. This supports the idea that the increases in G′ and G″ were due to rearrangements of the structure rather than the incorporation of free para-CMs or clusters (Mellema, Walstra, et al., 2002). The kinetics were more rapid when CMs were depleted in MCP, and slower when MCP-enriched. However, there was no direct relationship between gel pore size and G′ and G″ or tanδ for these three gels (Figs. 3, Figs. 4 and 6).

To observe the gel structure at the scale of para-CMs and assess the extent of fusion between the colloids, the gel samples were fixed for SEM observation 2 h after addition of the coagulant (Fig. 5D–F). The size of the elementary particles in the control and calcium-fortified gels corresponded to ~100 nm, close to the value expected for the diameter of CMs. However, the particles observed in the acidified gel were about twice this size. Before adding the coagulant, dynamic light scattering measurements revealed no difference in the hydrodynamic diameter of CMs between the three samples (Bauland, Bouchoux, Croguennec, Famelart, & Guyomarc'h, 2022). The larger particles observed in the acidified gel were probably the result of fusion between para-CMs, as suggested by Walstra and coworkers (Mellema, Walstra, et al., 2002; Walstra et al., 1985). Thus, the para-CMs depleted in MCP displayed a higher degree of fusion and the associated gel had a larger pore size. The structural evolution and extent of fusion of para-CMs were similar in both the control and calcium-fortified samples at least up to ~4 times the t_{gel}, which corresponded to the maximum observation period used here. This result was consistent with the gelation kinetics, which were also similar between these two gels up to ~5 times t_{gel}. However, the gel structure characterized in the present study could not fully explain the rheological properties of the gels, and particularly the greater elasticity of the calcium-fortified gel.

The aging of enzymatic milk gels has been studied in two frameworks, namely the mean field theory (Horne, 1996, 2003) and the fractal theory (Bremer, Van Vliet, & Walstra, 1989; Mellema, van Opheusden, & van Vliet, 2002). Under the mean field theory, CMs are considered as hard spheres, each able to form a defined number of bonds with their neighbors. After t_{gel}, the moduli of the gels increase and the aggregation of para-CMs continues until all potential bonds are established. Under the fractal theory, the moduli of individual CMs is infinitely large when compared to those of the gel, but the CMs are considered as soft enough to fuse after destabilization and aggregation. Walstra and coworkers (Mellema, Walstra, et al., 2002; Walstra et al., 1985) described the fusion between para-CMs as the driving force behind the rearrangement of enzymatic milk gel. The progressive fusion of colloids has also been observed in model colloidal systems, giving rise to universal aging features such as the continuous decline of the rate of gel aging over time

(Cipelletti, Manley, Ball, & Weitz, 2000; Joshi, 2014). The strengthening of inter-particle interactions would induce local shrinking of the colloidal gel and create regions of greater deformation because of the heterogeneous nature of the structure (Cipelletti et al., 2000). As revealed by numerical simulation, such localizations of force can induce bond breakings, whose consequences propagate over the gel network at distances larger than the pore size (Bouzid & Del Gado, 2018). These micro-compaction and micro-collapse events are cooperative in nature and give rise to aging kinetics that are relatively rapid in colloidal gels when compared to other glassy systems.

Based on rheological data, previous studies had proposed a relationship between the MCP content in CMs and their ability to fuse (Choi et al., 2007; Cooke & McSweeney, 2014; Mellema, Walstra, et al., 2002). The SEM images obtained here confirmed that CMs depleted in MCP had a higher degree of fusion at ~4 times t_{gel} whereas those enriched in MCP were not qualitatively different from the control condition at this point in aging (Fig. 5). Using atomic force microscopy, we were able to show that the Young modulus of CMs was positively correlated to their MCP content (Bauland et al., 2022), thus supporting the hypothesis that the ability of para-CMs to deform after contact is enhanced by reducing intra-micellar interactions.

In order to link the mineral content of CMs and the post-aggregation fusion ability of para-CMs, we assumed that the rate and extent of fusion were dependent on (i) the interaction strength between particles, which favors their fusion, and (ii) their rigidity, which opposes their fusion. Interactions between CMs, and particularly electrostatic repulsions, are highly dependent on the free Ca^{2+} that is in equilibrium with C-bound (Dalgleish, 1983; Horne & Lucey, 2014). Based on this, we propose a theoretical link between the partitioning of cations in CMs and the fusion ability of para-CMs. An increase in the MCP content would increase CM rigidity and oppose particle fusion, while an increase in C-bound would favor it by screening the repulsive charges of caseins. Following acidification at pH 6.0, both the increase in C-bound and the reduction in MCP in CMs promoted their fusion, explaining why larger particles were observed on SEM images of the acidified gel. After the addition of $CaCl_2$ to milk, the C-bound level also increased which promoted inter-particle interactions, but fusion was hindered by the increase in particle rigidity due to a higher MCP content. The fast fusion of para-CMs in the acidified gel probably resulted in the rapid development of an internal stress in the network that was forming and was still composed of thin strands. Under these conditions, stress relaxation soon resulted in a coarser gel, explaining the fast increase in large pore size (Fig. 6). By contrast, if particle fusion was hindered, aging kinetics were slower and gel pore size was smaller, as observed in the control and calcium-fortified samples (Figs. 2B and 6). The aging kinetics of the calcium-fortified gel slowed down when compared to the control gel at ~5 times the t_{gel}, (Fig. 2B), indicating that structural rearrangement was also hindered after a long aging time under these conditions. The kinetics of gel aging appeared to be clearly explained by the fusion ability of para-CMs. The dependence of para-CM fusion with their mineral content seemed consistent with the quantitative multivalent binding model for CM structure (Holt & Carver, 2022): C-bound would affect the charge of the CM surface while the MCP content, being the "cement" of the sub-structure, would affect the rigidity of the colloids.

The tanδ of the gels was anti-correlated to the MCP content in CMs over most of the frequency ranges tested (Fig. 3B), which was consistent with the relationship found in section 3.1 (Fig. 1). However, after a long aging time and at low frequency (Figs. 3B and 4), the calcium-fortified sample displayed greater elasticity whereas the difference between the control and acidified samples was smaller. No relationship was observed between the pore size of the gels or the size of the particles forming the gel (i.e. para-CMs or the result of their fusion) and the viscoelasticity of the gels. However, these parameters did not fully characterize the gel structure. The spatial distribution of para-CMs, or the type and number of bonds shared with neighbors, may be more relevant to explaining the rheological properties of the enzymatic gel. Structural heterogeneity has been reported to be a crucial parameter when explaining the frequency-dependent elasticity of colloidal gels (Rocklin, Hsiao, Szakasits, Solomon, & Mao, 2021). The higher elasticity observed with the calcium-fortified gel may have arisen from a combination of enhanced inter-particle interactions without excessive particle fusion, thus giving the gel a more homogenous structure. This idea was consistent with the delay in the decrease of the moduli after a long aging time for the calcium-fortified gel (Fig. 2B). The contribution of the interaction strength between colloids and the network structure to the rheological properties of colloidal gels is complex and remains an active field of research (Johnson, Zia, Moghimi, & Petekidis, 2019). In the present system, intra-micellar interactions involving MCP played an indirect but significant role in enzymatic gel rheology as they tuned the aging process and gel structure. In other colloidal systems, the deformability of particles has been shown to be crucial to explaining the degree of gel macro-syneresis, but the mechanical properties of single particles are often overlooked (Wu, Van Der Gucht, & Kodger, 2020).

Detailed characterization of the gel structure during formation and aging, using scattering techniques, would supply interesting supplementary information as these methods cover broader ranges of scales than microscopy techniques and are more appropriate to probing scaling laws and self-similar levels of organization.

4. Conclusion

We have shown that the two forms of cations (Ca^{2+} and Mg^{2+}) in CMs, i.e. directly bound to caseins (C-bound) and precipitated as micellar calcium phosphate (MCP), enable prediction of the rheological properties of enzymatic milk gel: a higher C-bound content increases G′ and G″ at 4 × t_{gel}, whereas a higher MCP content decreases tanδ, independently of gel firmness. These relationships agree with the findings of previous studies. They will be useful to predict the rheological properties of gels during cheese making as the gels in our study were formed under conditions close to those of processing in terms of coagulant level, the milk protein content or the temperature during gelation. To explain the relationship between the tanδ of the gels and the MCP content in CMs, we characterized a limited number of samples at longer timescales than those applied during cheese manufacture. We suggested that the C-bound and MCP contents had distinct effects on the fusion ability of para-CMs. The fusion rate of para-CMs and rearrangement of the gel network appeared to link the rheological and microscopic observations in a consistent manner, but the precise link between gel structure and its rheology will probably require a more detailed characterization of gel structure.

Author statement

Julien Bauland: Conceptualization, Writing - Original Draft, Data curation, Formal analysis, Investigation **Marie-Hélène Famelart**: Conceptualization, Investigation, Formal analysis, Writing - Review & Editing, Supervision **Marc Faiveley**: Conceptualization, Resources, Funding acquisition **Thomas Croguennec**: Conceptualization, Investigation, Writing - Review & Editing, Supervision, Funding acquisition, Project administration.

Acknowledgments

This work was funded by Chr-Hansen SAS and the ANRT. The authors are grateful to David Legland (BIBS platform, Nantes) for his help with the analysis of confocal images. We also thank Francis Gouttefangeas and the CMEBA-SCANMAT laboratory (Rennes 1 university) for acquiring SEM images, and Lazhar Benyahia (IMMM, Le Mans) for useful discussions.

Appendix A. Supplementary data

Supplementary data to this article can be found online at https://doi.org/10.1016/j.foodhyd.2022.107739.

References

Aime, S., Cipelletti, L., & Ramos, L. (2018). Power law viscoelasticity of a fractal colloidal gel. *Journal of Rheology, 62*(6), 1429. https://doi.org/10.1122/1.5025622

Bauland, J., Bouchoux, A., Croguennec, T., Famelart, M. H., & Guyomarc'h, F. (2022). Atomic force microscopy to assess the mechanical properties of individual casein micelles. *Food Hydrocolloids, 128*, 107577. https://doi.org/10.1016/j.foodhyd.2022.107577

Bauland, J., Famelart, M. H., Bouhallab, S., Jeantet, R., Roustel, S., Faiveley, M., et al. (2020). Addition of calcium and magnesium chlorides as simple means of varying bound and precipitated minerals in casein micelle: Effect on enzymatic coagulation. *Journal of Dairy Science, 103*(11), 9923–9935. https://doi.org/10.3168/jds.2020-18749

Bonfanti, A., Kaplan, J. L., Charras, G., & Kabla, A. (2020, July 8). *Fractional viscoelastic models for power-law materials. Soft Matter*. Royal Society of Chemistry. https://doi.org/10.1039/d0sm00354a

Bouzid, M., & Del Gado, E. (2018). Elastic relaxation and response to deformation of soft gels. *ACS Symposium Series, 1296*, 211–225. https://doi.org/10.1021/bk-2018-1296.ch011. American Chemical Society.

Bremer, L. G. B., Van Vliet, T., & Walstra, P. (1989). Theoretical and experimental study of the fractal nature of the structure of casein gels. *Journal of the Chemical Society, Faraday Transactions 1: Physical Chemistry in Condensed Phases, 85*(10), 3359–3372. https://doi.org/10.1039/F19898503359

Choi, J., Horne, D. S., & Lucey, J. A. (2007). Effect of insoluble calcium concentration on rennet coagulation properties of milk. *Journal of Dairy Science, 90*(6), 2612–2623. https://doi.org/10.3168/jds.2006-814

Cipelletti, L., Manley, S., Ball, R. C., & Weitz, D. A. (2000). Universal aging features in the restructuring of fractal colloidal gels. *Physical Review Letters, 84*(10), 2275–2278. https://doi.org/10.1103/PhysRevLett.84.2275

Cooke, D. R., & McSweeney, P. L. H. (2014). The influence of alkaline earth metal equilibria on the rheological properties of rennet-induced skim milk gels. *Dairy Science & Technology, 94*(4), 341–357. https://doi.org/10.1007/s13594-014-0166-5

Dalgleish, D. G. (1983). Coagulation of renneted bovine casein micelles: Dependence on temperature, calcium ion concentration and ionic strength. *Journal of Dairy Research, 50*(3), 331–340. https://doi.org/10.1017/S0022029900023165

De Kruif, C. G. (1999). Casein micelle interactions. *International Dairy Journal, 9*, 183–188. https://doi.org/10.1016/S0958-6946(99)00058-8. Elsevier.

Famelart, M. H., Tomazewski, J., Piot, M., & Pezennec, S. (2004). Comprehensive study of acid gelation of heated milk with model protein systems. *International Dairy Journal, 14*(4), 313–321. https://doi.org/10.1016/J.IDAIRYJ.2003.10.009

Fox, P. F., & Brodkorb, A. (2008). The casein micelle: Historical aspects, current concepts and significance. *International Dairy Journal, 18*(7), 677–684. https://doi.org/10.1016/J.IDAIRYJ.2008.03.002

Gaucheron, F. (2004). *Minéraux et Produits Laitiers. Minéraux et produits laitiers*. Tec & Doc).

Holt, C. (1992). Structure and stability of bovine casein micelles. *Advances in Protein Chemistry, 43*(C), 63–151. https://doi.org/10.1016/S0065-3233(08)60554-9

Holt, C. (2016). Casein and casein micelle structures, functions and diversity in 20 species. *International Dairy Journal, 60*, 2–13. https://doi.org/10.1016/j.idairyj.2016.01.004

Holt, C., & Carver, J. A. (2022). Quantitative multivalent binding model of the structure, size distribution and composition of the casein micelles of cow milk. *International Dairy Journal, 126*, 105292. https://doi.org/10.1016/j.idairyj.2021.105292

Holt, C., Carver, J. A., Ecroyd, H., & Thorn, D. C. (2013). Invited review: Caseins and the casein micelle: Their biological functions, structures, and behavior in foods. *Journal of Dairy Science, 96*(10), 6127–6146. https://doi.org/10.3168/JDS.2013-6831

Holt, C., Davies, D. T., & Law, A. J. R. (1986). Effects of colloidal calcium phosphate content and free calcium ion concentration in the milk serum on the dissociation of bovine casein micelles. *Journal of Dairy Research, 53*, 557. https://doi.org/10.1017/S0022029900033082, 04.

Horne, D. S. (1996). Aspects of scaling behaviour in the kinetics of particle gel formation. *Journal de Chimie Physique et de Physico-Chimie Biologique, 93*(5), 977–986. https://doi.org/10.1051/jcp/1996930977

Horne, D. S. (1998). Casein interactions: Casting light on the black boxes, the structure in dairy products. *International Dairy Journal, 8*(3), 171–177. https://doi.org/10.1016/S0958-6946(98)00040-5

Horne, D. S. (2003). Casein micelles as hard spheres: Limitations of the model in acidified gel formation. *Colloids and Surfaces A: Physicochemical and Engineering Aspects, 213*(2–3), 255–263. https://doi.org/10.1016/S0927-7757(02)00518-6

Horne, D. S. (2020). Casein micelle structure and stability. In *Milk proteins* (pp. 213–250). Elsevier. https://doi.org/10.1016/b978-0-12-815251-5.00006-2.

Horne, D. S., & Lucey, J. A. (2014). Revisiting the temperature dependence of the coagulation of renneted bovine casein micelles. *Food Hydrocolloids, 42*, 75–80. https://doi.org/10.1016/j.foodhyd.2013.12.021

Horne, D. S., & Lucey, J. A. (2017). Rennet-Induced coagulation of milk. In*Cheese: Chemistry, Physics and Microbiology* (4th ed., Vol. 1, pp. 115–143). Elsevier Inc. https://doi.org/10.1016/B978-0-12-417012-4.00005-3.

Johnson, L. C., Zia, R. N., Moghimi, E., & Petekidis, G. (2019). Influence of structure on the linear response rheology of colloidal gels. *Journal of Rheology, 63*(4), 583–608. https://doi.org/10.1122/1.5082796

Joshi, Y. M. (2014). June 9). Dynamics of colloidal glasses and gels. Annual review of chemical and biomolecular engineering. *Annual Reviews*. https://doi.org/10.1146/annurev-chembioeng-060713-040230

Legland, D., Devaux, M. F., Bouchet, B., Guillon, F., & Lahaye, M. (2012). Cartography of cell morphology in tomato pericarp at the fruit scale. *Journal of Microscopy, 247*(1), 78–93. https://doi.org/10.1111/j.1365-2818.2012.03623.x

Lê, S., Josse, J., & Husson, F. (2008). FactoMineR: An R package for multivariate analysis. *Journal of Statistical Software, 25*(1), 1–18. https://doi.org/10.18637/jss.v025.i01

McMahon, D. J., & Oommen, B. S. (2013). Casein micelle structure, functions, and interactions. In *Advanced dairy chemistry: Volume 1A: Proteins: Basic aspects* (4th ed., pp. 185–209). Boston, MA: Springer US. https://doi.org/10.1007/978-1-4614-4714-6_6.

Mekmene, O., Le Graët, Y., & Gaucheron, F. (2009). A model for predicting salt equilibria in milk and mineral-enriched milks. *Food Chemistry, 116*(1), 233–239. https://doi.org/10.1016/J.FOODCHEM.2009.02.039

Mellema, M., Van Opheusden, J. H. J., & Van Vliet, T. (1999). Relating colloidal particle interactions to gel structure using Brownian dynamics simulations and the Fuchs stability ratio. *The Journal of Chemical Physics, 111*(13), 6129–6135. https://doi.org/10.1063/1.479956

Mellema, M., van Opheusden, J. H. J., & van Vliet, T. (2002). Categorization of rheological scaling models for particle gels applied to casein gels. *Journal of Rheology, 46*(1), 11–29. https://doi.org/10.1122/1.1423311

Mellema, M., Walstra, P., van Opheusden, J. H., & van Vliet, T. (2002). Effects of structural rearrangements on the rheology of rennet-induced casein particle gels. *Advances in Colloid and Interface Science, 98*(1), 25–50. https://doi.org/10.1016/S0001-8686(01)00089-6

Mishra, R., Govindasamy-Lucey, S., & Lucey, J. A. (2005). Rheological properties of rennet-induced gels during the coagulation and cutting process: Impact of processing conditions. In *Journal of Texture studies §* (Vol. 36)John Wiley & Sons, Ltd. https://doi.org/10.1111/j.1745-4603.2005.00011.x, 10.1111.

Ong, L., Dagastine, R. R., Kentish, S. E., & Gras, S. L. (2010). The effect of milk processing on the microstructure of the milk fat globule and rennet induced gel observed using confocal laser scanning microscopy. *Journal of Food Science, 75*(3), E135–E145. https://doi.org/10.1111/j.1750-3841.2010.01517.x

Philippe, M., Le Graët, Y., & Gaucheron, F. (2005). The effects of different cations on the physicochemical characteristics of casein micelles. *Food Chemistry, 90*(4), 673–683. https://doi.org/10.1016/J.FOODCHEM.2004.06.001

Rocklin, D. Z., Hsiao, L., Szakasits, M., Solomon, M. J., & Mao, X. (2021). Elasticity of colloidal gels: Structural heterogeneity, floppy modes, and rigidity. *Soft Matter, 17*(29), 6929–6934. https://doi.org/10.1039/d0sm00053a

Udabage, P., McKinnon, I. R., & Augustin, M. A. (2001). Effects of mineral salts and calcium chelating agents on the gelation of renneted skim milk. *Journal of Dairy Science, 84*(7), 1569–1575. https://doi.org/10.3168/jds.S0022-0302(01)74589-4

Vilet, T. van, Roefs, S. P. F. M., Zoon, P., & Walstra, P. (1989). Rheological properties of casein gels. *Journal of Dairy Research, 56*(3), 529–534. https://doi.org/10.1017/S0022029900029022

van Vliet, T., van Dijk, H. J. M. M., Zoon, P., & Walstra, P. (1991). Relation between syneresis and rheological properties of particle gels. *Colloid & Polymer Science, 269*(6), 620–627. https://doi.org/10.1007/BF00659917

Walstra, P., van Dijk, H., & Geurts, T. (1985). The syneresis of curd. 1. General considerations and literature review. *Netherlands Milk and Dairy Journal, 39*(4), 209–246. Retrieved from https://agris.fao.org/agris-search/search.do?recordID=NL8600289.

Wang, Q., Holt, C., Nylander, T., & Ma, Y. (2020). Salt partition, ion equilibria, and the structure, composition, and solubility of micellar calcium phosphate in bovine milk with added calcium salts. *Journal of Dairy Science, 103*(11), 9893–9905. https://doi.org/10.3168/jds.2020-18829

Wu, Q., Van Der Gucht, J., & Kodger, T. E. (2020). Syneresis of colloidal gels: Endogenous stress and interfacial mobility drive compaction. *Physical Review Letters, 125*(20), 1–6. https://doi.org/10.1103/PhysRevLett.125.208004

Zoon, P. (1988). PhD thesis. Wageningen Agricultural University,The Netherlands.

Zoon, P., Roefs, S. P. F. M., de Cindio, B., & van Vliet, T. (1990). Rheological properties of skim milk gels at various temperatures; interrelation between the dynamic moduli and the relaxation modulus. *Rheologica Acta, 29*(3), 223–230. https://doi.org/10.1007/BF01331358

Zoon, P., van Vliet, T., & Walstra, P. (1988). Rheological properties of rennet-induced skim milk gels 3. The effect of calcium and phosphate. *Netherlands Milk and Dairy Journal, 42*(3), 271–294.